ELSEVIER

Journal of Magnetism and Magnetic Materials 232 (2001) 71–83

Journal of magnetism and magnetic materials

www.elsevier.com/locate/jmmm

Magnetic properties of nanocrystalline $CoFe_2O_4$ powders prepared at room temperature: variation with crystallite size

M. Rajendran[a], R.C. Pullar[a], A.K. Bhattacharya[a,*], D. Das[b], S.N. Chintalapudi[b], C.K. Majumdar[c]

[a] *Warwick Process Technology Group, School of Engineering, University of Warwick, Coventry CV4 7AL, UK*
[b] *Inter-University Consortium for DAE Facilities, Bidhan Nagar, Calcutta 700 091, India*
[c] *PAMU, Indian Statistical Institute, Calcutta 700 035, India*

Received 15 August 2000; received in revised form 14 December 2000

Abstract

The magnetic properties of nanocrystalline $CoFe_2O_4$ powders prepared by a redox process at room temperature have been studied by vibrating sample magnetometer (VSM). The average crystallite size of the powders varied from 6 to 20 nm by changing the synthesis conditions and the corresponding saturation magnetisation (M_s) value ranged from 9 to 38 emu g^{-1}. On heating, the crystallite size increased with corresponding increase in M_s values. At 1073 K all samples achieved M_s values close to 73 emu g^{-1}. On increasing the crystallite size, the coercivity (H_c) increased passed through a maximum and dropped. Cobalt ferrite powder with an average crystallite size of 6 nm prepared at room temperature achieved desirable values of $M_s = 60$ emu g^{-1} and $H_c = 1.42$ kOe after thermal annealing at 973 K. The Mössbauer spectra were recorded for $CoFe_2O_4$ having a range of crystallite sizes at room temperature and at low temperatures down to 40 K. The magnetic and Mössbauer results are provided for nanocrystalline $CoFe_2O_4$ as a function of crystallite size and measurement temperature.

Keywords: Nanocrystalline; Cobalt ferrite; Superparamagnetism; Mössbauer spectra

1. Introduction

Cobalt ferrite, $CoFe_2O_4$ crystallises in a partially inverse spinel structure represented as $(Co_x^{2+}Fe_{1-x}^{3+})[Co_{1-x}^{2+}Fe_{1+x}^{3+}]O_4$ where x depends on thermal history [1]. It is ferrimagnetic with a Curie temperature (T_c) around 520°C and shows a relatively large magnetic hysteresis which distinguishes it from the rest of the spinel ferrites. Magnetic measurements on magnetic fluids containing nanoparticles of cobalt ferrite (10^{-2}–10^{-3} M) dispersed in organic solvents [2] and nanocrystalline powders prepared by hydroxide precipitation [3–5] have been studied earlier. In magnetic fluids, it has been seen that for particles above 3 nm the saturation magnetisation remains constant at about 30 emu g^{-1}which is considerably less than the bulk value. On the other hand, 5 nm particles produced by precipitation techniques were found to have a saturation magnetisation less than 14.5 emu g^{-1} [3]. This could be due to the

*Corresponding author. Tel.: +1-44-1203-524201; fax: +1-44-1203-528998.
E-mail address: ashokbhattacharya@warwick.ac.uk (A.K. Bhattacharya).

0304-8853/01/$ - see front matter
PII: S0304-8853(01)00151-2

two studies employing different preparation techniques.

In our laboratory, a redox method has been developed to prepare dispersible nanocrystalline oxides at room temperature [6]. The method employs inexpensive inorganic reagents and requires only a short duration of about 30 min to form spinel ferrites. In order to get a better understanding of the effect of crystallite size upon the magnetic property of nanocrystalline $CoFe_2O_4$, a systematic study has been carried out and the results are presented in this paper.

2. Experimental

2.1. Materials

All the chemicals and reagents used were of high purity and commercially available (Aldrich, UK)

Cobalt (II) chloride hexahydrate (98%), iron (II) chloride tetrahydrate (99%), sodium hydroxide (99%) were used as starting materials. The details of the preparation are described elsewhere [6]. In brief, aqueous metal chloride solutions of 0.1–1.0 M concentrations were mixed together such that $[Co^{2+}]:[Fe^{2+}]=1:2$ followed by simultaneous oxidative precipitation under controlled conditions using aqueous NaOH and H_2O_2. Fine cobalt ferrite powder was instantly formed by the oxidative precipitation process, which was then isolated, washed with water and dried under reduced pressure of 10^{-2} Torr. For a 0.4 M metal ion concentration, fine cobalt ferrite powders having an average crystallite size of 6 nm was obtained.

The resultant $CoFe_2O_4$ powder was designated as 6 nm sized $CoFe_2O_4$. Several portions were made from this and each of the portions was thermally annealed to increasingly higher temperatures.

2.2. Characterisation

(a) *X-ray powder diffraction (XRD) measurements:* The XRD pattern of the as prepared sample and the patterns for samples heated to various temperatures were recorded in the region $2\theta = 10$–90° in steps of $0.1^\circ\,\mathrm{min}^{-1}$ on a Philips diffractometer (Model PW 1710) using Cu K_α radiation. Cell parameters were calculated and further refined using linear regression procedures (Philips APD 1700 software) applied to the measured peak positions of all major reflections up to $2\theta = 10$–90°. Accurate measurements of peak shift were carried out on selected low angle reflections.

(b) *Crystallite size measurements:* Crystallite sizes were determined from the full-width at half-maximum (FWHM) of the strongest reflection, the (3 1 1) peak using the Scherrer equation [7]

$$D = k\lambda/\beta_{1/2}\cos\theta,$$

where D is the crystallite size, k is a shape function for which a value of 0.9 is used, λ is the wavelength of the radiation (Cu $K_\alpha = 0.154178$ nm) and θ is the angle of incidence. The value of $\beta_{1/2}$ was determined from the experimental integral peak width (FWHM) by applying standard correction for the instrumental broadening.

(c) *Surface area measurements:* Specific surface area and pore size distribution measurements were performed on a micromeritics, accelerated surface area and porosimetry system (ASAP 2000). The samples were degassed at 200°C for sixth prior to the measurement. The measurement is based on the Brunauer–Emmett–Teller (BET) principle which can be represented as [8]

$$(P/P_s)/[V(1-(P/P_s))] = (1/V_mC) + [(C-1)V_mC](P/P_s),$$

where V is the volume of gas adsorbed at pressure P, P_s is the saturation pressure, i.e., the vapour pressure of liquid gas at the adsorbing temperature, V_m is the volume of gas required to form the monolayer and C is a constant related to the energy of adsorption. A plot of $P/V\ (P_s - P)$ against P/P_s gives a straight line with an intercept and slope of $1/V_mC$, and $(C-1)/V_mC$, respectively. The value of V_m is extracted from a series of experiments made by varying the pressure of the adsorbate, N_2.

(d) *Porosity measurements:* In order to evaluate the type of pore and pore volume distribution, adsorbtion–desorption isotherms for the cobalt ferrite powders were measured on the

Micromeritics equipment. In a typical experiment, the volume of nitrogen adsorbed in $cm^3 g^{-1}$ at STP was monitored against the relative pressure (P/P_s), ranging from 0 to 1, and the relative pressure was reversed to measure the volume of gas desorbed. A plot of volume adsorbed and desorbed against relative pressure gives an isotherm with characteristic hysteresis from which the type of pore and pore size distribution were determined.

(e) *Magnetic measurements:* Magnetisation measurements were carried out on a known quantity of randomly dispersed particles set and cured in a polymer matrix (methyl methacrylate-styrene resin). An Oxford Research Instruments Maglab vibrating sample magnetometer (VSM) was used to obtain the $M-H$ loop at room temperature and low temperatures down to 20 K. The instrument consists of a helium cooled superconducting magnet to render field strengths of up to 12 T.

(f) *Mössbauer measurements:* Mössbauer spectra were acquired with a standard PC based spectrometer operating in constant acceleration mode using a multichannel analyser. A 10 mCi ^{57}Co in Rh matrix was used as a radioactive source and the spectrometer was calibrated with a 12 μm thick high purity iron foil. Low-temperature data down to 40 K were recorded by mounting the sample in a closed cycle helium refrigerator (model DMX 20 from APD Cryogenics Inc.) [9]. The experimental data were analysed with a standard least squares fitting program assuming Lorentzian line shapes.

(g) *Thermogravimetric and differential thermal analysis (TG-DTA) measurements:* Simultaneous TG-DTA measurements were performed on a commercial equipment, STA 1500, Rheometric scientific in static air. The rate of heating was set at $20^{\circ}C\,min^{-1}$ and the analysis was performed in the temperature range 20–850°C.

3. Results and discussion

Fig. 1(a) shows the powder XRD pattern of the sample prepared at room temperature. The XRD reflections are characteristic of cubic spinel structure and the absence of extra reflections in the diffraction pattern ensures the phase purity. The

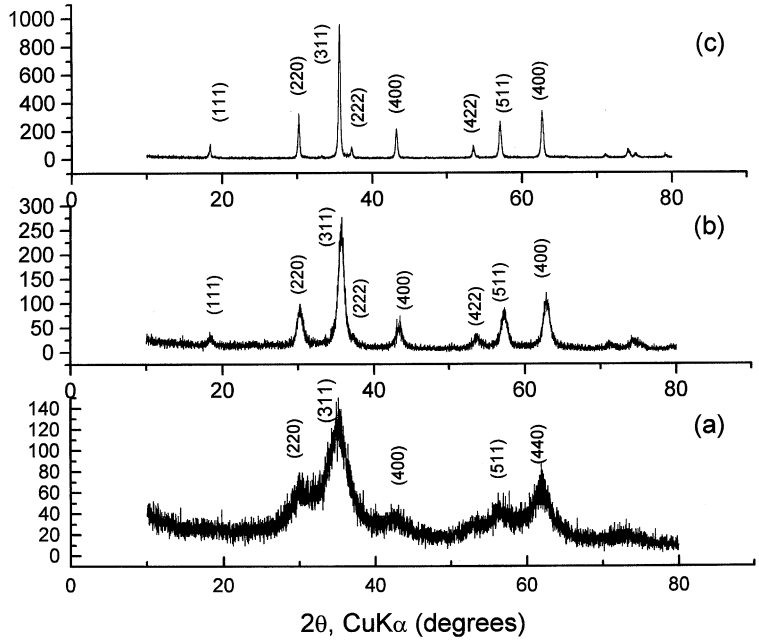

Fig. 1. Powder XRD pattern of (a) 6 nm (b) 20 nm and (c) sample annealed at 973 K.

oxyhydroxide phase forms as an intermediate in the present process which converts to spinel under controlled conditions. The interplanar reflections of the oxyhydroxide and spinel phase are closely related. However, the (1 1 1) reflection is characteristic of oxide spinel phase which distinguishes it from the oxyhydroxide phase. Presence of oxyhydroxide phase is expected to show a weight-loss upon heating the sample to high temperature of 1073 K. Since no appreciable weight-loss was registered when the sample was heated to 1073 K, the absence of oxyhydroxide phase became evident. Clearly, if there were any oxyhydroxide phase present, TG-DTA curves should have indicated weight-loses and corresponding heat changes due to the decomposition of these phases. The nanocrystallinity of the sample was inferred from the relatively broad diffraction peaks. The average crystallite size of the room temperature prepared sample was determined to be 6 nm from the prominent (3 1 1) reflection of the diffraction pattern. The unit cell parameter was determined to be $a_0 = 8.392$ Å. The values of inter-planar distances and the unit cell parameter were in agreement with the reported values (JCPDS 22-1086 $CoFe_2O_4$) [10]. Absence of lattice strain was inferred from the following relation: $\beta_s = (\Delta d/d)\tan\theta$ where, β_s is the lattice strain, d is the lattice constant and Δd is the change in lattice constant because of strain [11]. For twice the increase in the concentration of metal salt solutions to 0.8 M, 20 nm sized $CoFe_2O_4$ powder was obtained and the corresponding XRD pattern is shown in Fig. 1(b). Fig. 1(c) is the XRD pattern of the $CoFe_2O_4$ after thermal annealing at 973 K, showing relatively sharp XRD reflections. The crystallite size increases when the room temperature prepared 6 nm sized $CoFe_2O_4$ is heated to increasingly higher temperatures. Fig. 2 displays the variation of crystallite size as a function of thermal annealing. As seen from the plot, the crystallite size increases significantly when the sample is heated above 873 K.

The porosity and pore-size distribution in $CoFe_2O_4$, were determined from adsorption–desorption isotherms. A typical adsorption–desorption isotherm of the room temperature prepared $CoFe_2O_4$ powder is shown in Fig. 3(a). It can be observed that the sample adsorbs 35 $cm^3 g^{-1}$ of nitrogen at a relative pressure (p/p_0) of 0.05. As the relative pressure was increased to 0.5, there was a gradual and linear increase in the amount of nitrogen adsorbed to about 67 $cm^3 g^{-1}$, i.e., the volume of nitrogen

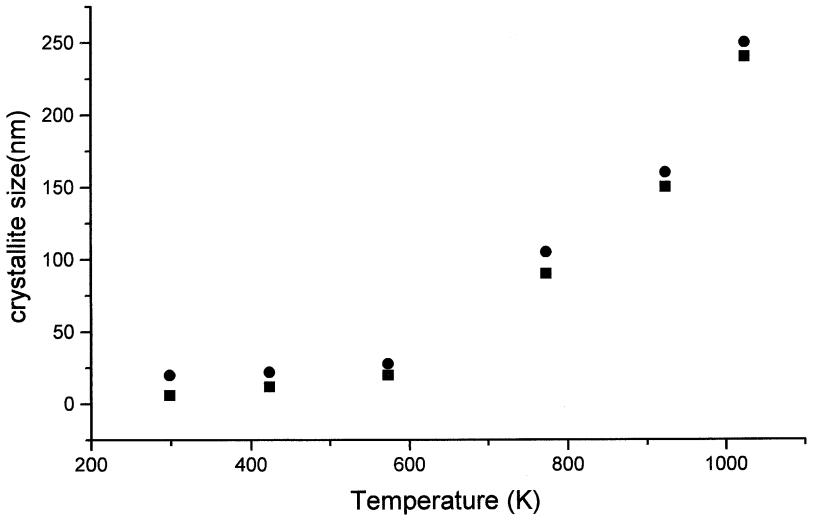

Fig. 2. Variation of crystallite size against annealing temperature. The square and circle represent 6 and 20 nm sized samples respectively, prepared at room temperature.

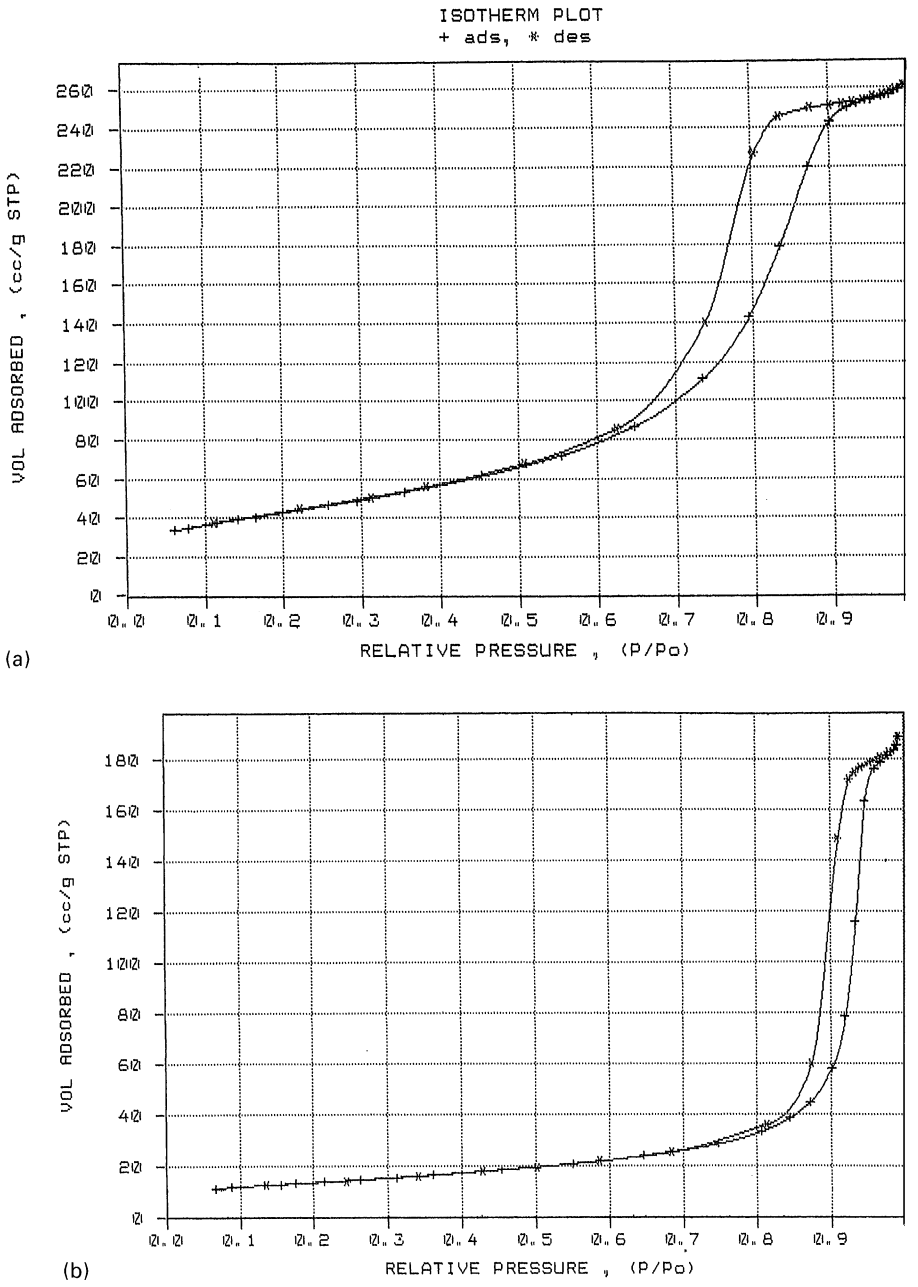

Fig. 3. Adsorption-desorption isotherms of (a) 6 nm sized $CoFe_2O_4$ and (b) 20 nm sized $CoFe_2O_4$.

adsorbed doubled compared to the initial value. When the relative pressure was increased above 0.6, there was a dramatic increase in the amount of nitrogen adsorbed to 250 $cm^3 g^{-1}$. Beyond this point, a saturation behaviour was seen in the adsorption isotherm. The desorption isotherm was recorded by gradually decreasing the relative pressure from 1 to 0.05. At higher relative

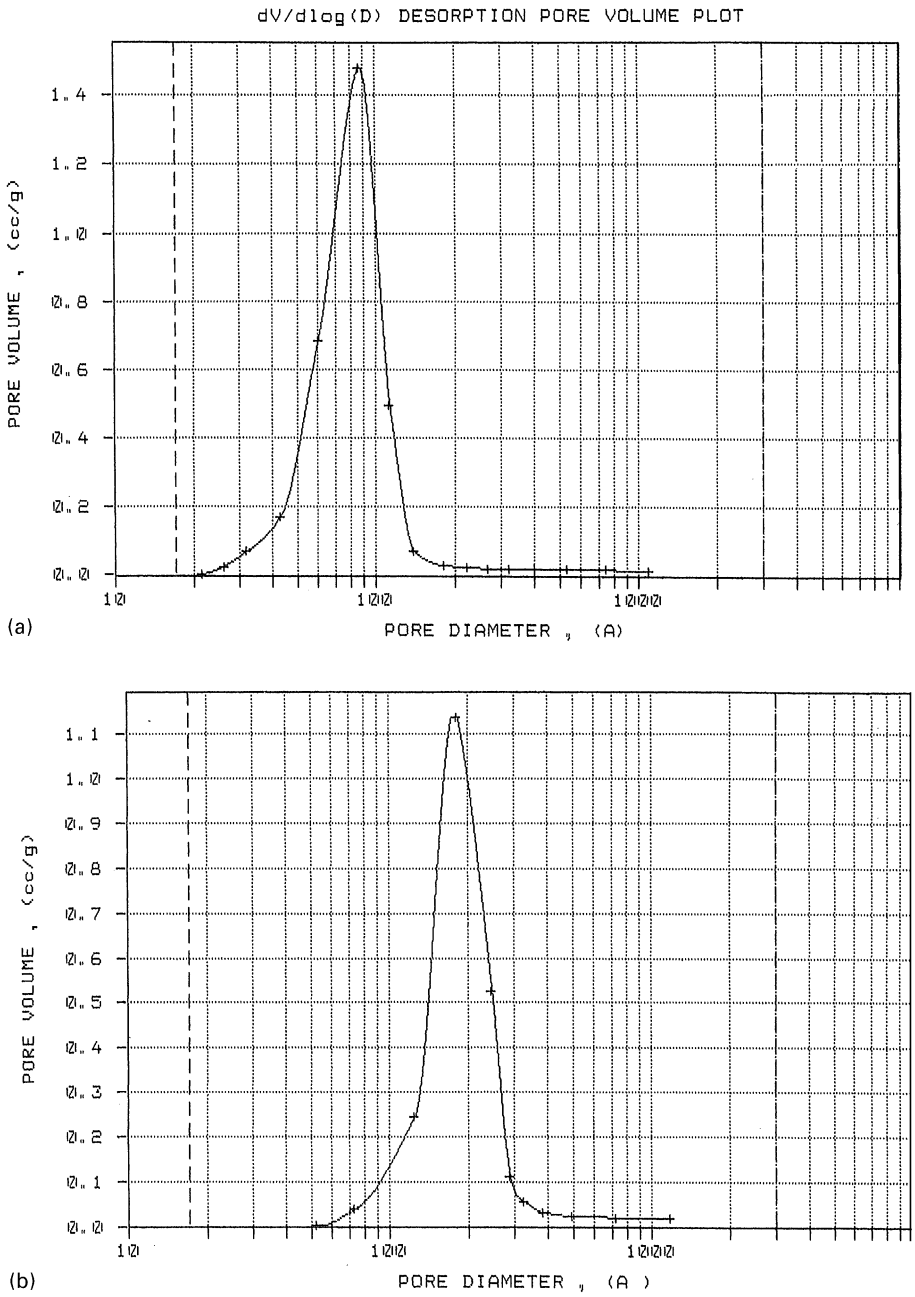

Fig. 4. Pore-size distribution of $CoFe_2O_4$ powders (a) 6 nm sized and (b) 20 nm sized.

pressures, the desorption branch did not follow the adsorption branch because of the capillary condensation of nitrogen resulting in a hysteresis. For instance, at a relative pressure of 0.8, the volume of nitrogen adsorbed was $227\,cm^3\,g^{-1}$ whilst, the volume desorbed was only $142\,cm^3\,g^{-1}$. The appearance of a hysteresis is a clear indication of porosity in the sample. The shape and width of the

hysteresis suggests the presence of cylindrical pores. However, below $p/p_0 = 0.5$, both the adsorption and desorption branches merge together to show reversibility. Fig. 3(b) is a representative adsorption–desorption isotherm of a sample heated to a higher temperature of 873 K. It is evident in this case that the hysteresis is relatively narrower and the adsorption–desorption branches merge at a higher relative pressure of 0.75. The magnitude of decrease in the volume of gas adsorbed reveals a lower surface area.

The particle size of room temperature prepared $CoFe_2O_4$ was calculated from the BET surface area using the relation, $S_{BET} = 6/(\varrho x d_{av})$ where, S_{BET} is the surface area of $CoFe_2O_4$ ($154\,m^2\,g^{-1}$), ϱ is the density (5.274) and d_{av} is the average particle size which is determined to be 7.4 nm. On heating the sample to 873 K, the surface area decreases to $47\,m^2\,g^{-1}$. From this, an average particle size of 24 nm was estimated. These values are comparable to the crystallite sizes determined from the XRD measurements. The pore-size distributions in as prepared $CoFe_2O_4$ and the sample annealed at 873 K were measured from the desorption pore volume plot shown in Figs. 4(a) and (b), respectively. The plot shows a single feature characteristic of relatively narrow size distribution of pores.

The variation in saturation magnetisation (M_s) with average crystallite size is shown in Fig. 5. For the 6 nm sized $CoFe_2O_4$ the M_s value was measured to be $9\,emu\,g^{-1}$ at 12 T. The magnetisation did not show saturation even at a field of 12 T for this sample as seen from the inset. The sample is found to be superparamagnetic from the complete reversibility of the $M-H$ curve recorded at room temperature. Increasing the average crystallite size to 20 nm the M_s value increased to $50\,emu\,g^{-1}$. In this case, the sample exhibited a narrow hysteresis which is seen in Fig. 5(b). It is also evident from the magnetisation curve that the saturation is not achieved. The crystallite size of the sample was increased to about 50 nm by heating the 6 nm sized sample to 1073 K. The magnetisation, in this case, was found to be $73\,emu\,g^{-1}$ and a prominent hysteresis was observed which is shown in Fig. 5(c). The M_s values measured for the samples are lower than the bulk value of $75\,emu\,g^{-1}$. The M_s values increased with annealing temperature as a result of crystallite growth, exceeded $70\,emu\,g^{-1}$ after thermal annealing at 1073 K. The variation of M_s values as a function of annealing temperature is shown in Fig. 6. It is clearly seen that the M_s values increase with annealing temperature.

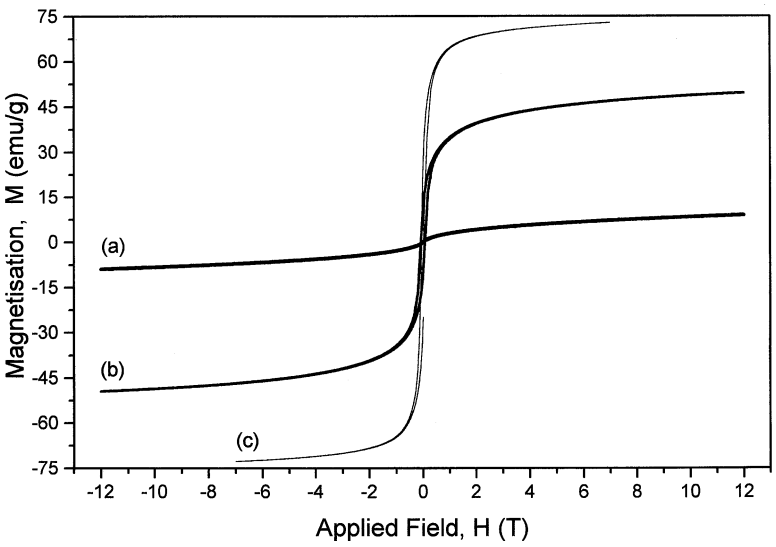

Fig. 5. $M-H$ plots of $CoFe_2O_4$ (a) 6 nm sized (b) 20 nm sized and (c) 200 nm sized crystallites.

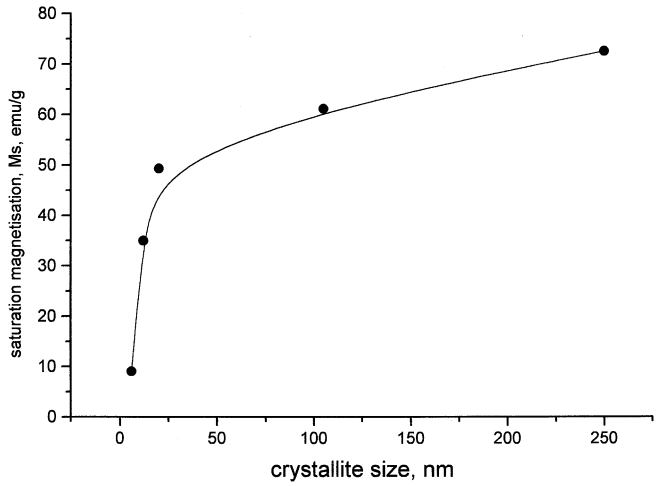

Fig. 6. Variation of saturation magnetisation (M_s) against crystallite size of $CoFe_2O_4$.

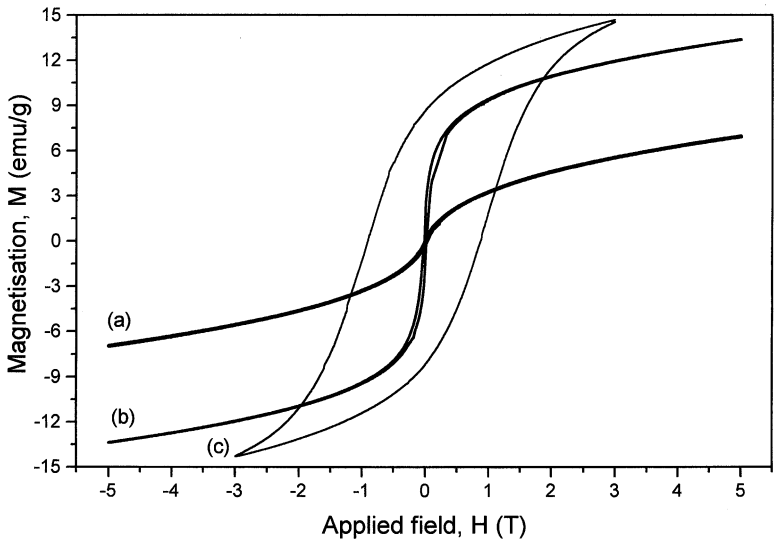

Fig. 7. $M-H$ plots of 6 nm sized $CoFe_2O_4$ at (a) 300 K, (b) 150 K and (c) 20 K.

The variation in magnetisation as a function of temperature is shown in Fig. 7 for 6 nm sized $CoFe_2O_4$ powders. The $M-H$ curves were obtained at 300, 150 and 20 K upto a field strength of 5 T. The sample exhibited superparamagnetic behaviour at 300 K and the behaviour is shown in Fig. 7(a). When the temperature was lowered to 150 K, the sample exhibited a narrow hysteresis as shown in Fig. 7(b) and the M_s value increased to 13 emu g^{-1}. For a further decrease in temperature to 20 K, the hysteresis was pronounced and the hysteresis loop opened up at 3 T. The M_s, M_r and H_c values measured from the $M-H$ curves at 300, 150 and 20 K are listed in Table. 1.The hysteresis

Table 1
Magnetic properties of nanocrystalline $CoFe_2O_4$ samples

Crystallite size of $CoFe_2O_4$ (nm)	Magnetic characteristics								
	300 K			150 K			20 K		
	M_s (emu g^{-1})	M_r (emu g^{-1})	H_c (T)	M_s (emu g^{-1})	M_r (emu g^{-1})	H_c (T)	M_s (emu g^{-1})	M_r (emu g^{-1})	H_c (T)
6	9	0.55	0.0	13.4	1.33	0.012	14.7	8.7	0.91
12	35	5.2	0.0	—	—	—	—	—	—
20	49.3	6.8	0.0	—	—	—	—	—	—
105	61.06	21.3	0.12	71.3	42.0	0.56	69.6	50.2	1.39
Above 200 nm	72.5	25.5	0.58	—	—	—	—	—	—

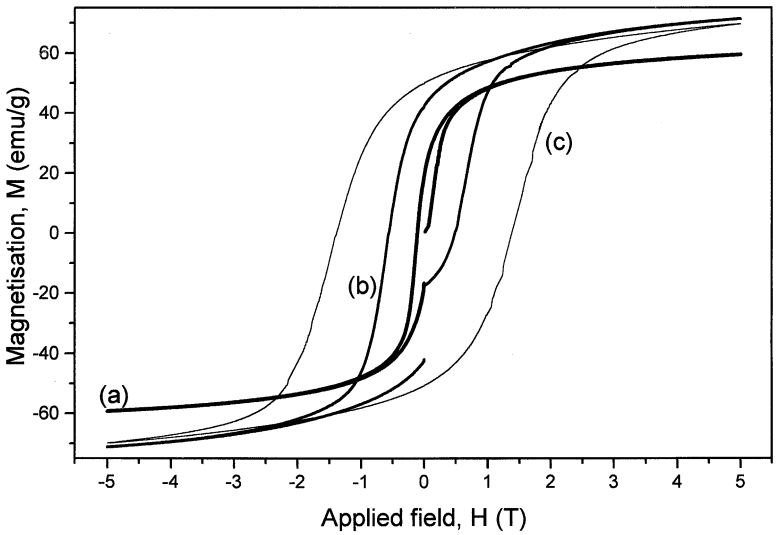

Fig. 8. $M-H$ plots of 200 nm sized $CoFe_2O_4$ at (a) 300 K, (b) 150 K and (c) 20 K.

opened up to give a coercivity of 0.012 T at 150 K which increased to 0.91 T at 20 K.

Similarly, the 6 nm sized sample prepared at room temperature was thermally annealed to 973 K and the variation in magnetisation was studied at 300, 150 and 20 K. The typical $M-H$ curves are shown in Fig. 8. At 300 K, the sample exhibited M_s value of 61 emu g^{-1} and H_c value of 0.12 T. The corresponding remanance (M_r) at 300 K was measured to be 21 emu g^{-1}. These values increased considerably on cooling the sample to lower temperatures. At 150 K, the M_s, M_r and H_c values increased to 71, 42 emu g^{-1} and 0.56 T, respectively. A pronounced increase in these values to $M_s = 70$ emu g^{-1}, $M_r = 49$ emu g^{-1} and $H_c = 1.42$ T was seen at 20 K. The results are summarised in Table 1.

The variation of coercivity (H_c) with the crystallite size at room temperature is shown in Fig. 9. The average crystallite size of the sample was varied from 6 nm to higher values by thermal annealing. The H_c value was determined from the $M-H$ hysteresis recorded at room temperature. As seen from the plot the coercivity increased to show a maximum and dropped. The coercivity maximum is centred around 175 nm crystallite size and the corresponding annealing temperature was 973 K. A further increase in crystallite size above 200 nm lowers the coercivity.

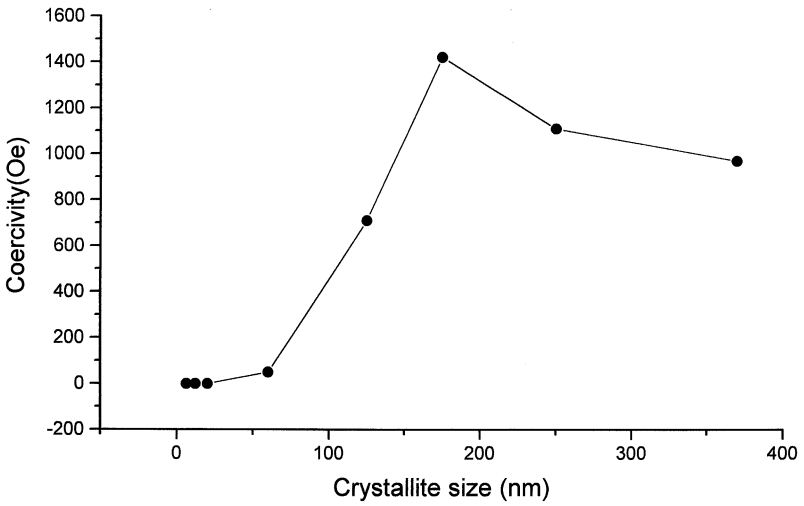

Fig. 9. Variation of coercivity (H_c) against crystallite size.

The lower M_s values associated with nanocrystalline $CoFe_2O_4$ powders could be attributed to the structural distortions in the surface compared to the bulk [12]. It can be understood by considering the transition metal ions as having a net magnetic moment which interact through the oxygen atoms in spinel lattice resulting in a situation where the magnetic moments of both A- and B-site ions are aligned. The alignment is such that A–A and B–B are parallel, whilst A–B is antiparallel to give a ferrimagnetic ordering. The net magnetic moment per formula unit can be calculated from the distribution of metal ions over these sites. The net magnetic moment is reduced in ultrafine particles as the sample has significantly large surface to volume ratio. Thus, a large proportion of metal ions are in structurally distorted particle surface, wherein, the bond lengths and bond angles would be different compared to the bulk to give reduced magnetic moments. It is also likely that the cation site occupancy in nanosized $CoFe_2O_4$ could be different from the bulk to give reduced magnetic moment. Further work is underway to identify the amount of Fe^{3+} in terahedral and octahedral sites in the spinel structure. Our earlier work on metal clusters has suggested that the behaviour of nanoparticles would be quite different from that of the bulk.

The saturation magnetisation (M_s) well below the blocking temperature can be related to the anisotropy constant (K) and initial susceptibility (χ_{in}) by the following equation [3,13]: $3K = M_s^2/(\chi_{in})$; the anisotropy constant estimated from this relation using maximal measured magnetisation at 40 K and measured susceptibility at the same temperature gives a value of 1.4×10^6 erg cm^{-3}, which is lower than the reported cubic anisotropy constant.

Mössbauer spectra of $CoFe_2O_4$ samples having different crystallite sizes were recorded at room temperature and representative spectra are shown in Fig. 10. As seen from Fig. 10(a) the 6 nm sized sample gives a doublet pattern originating from nuclear quadruple splitting of ^{57}Fe, and there are no magnetic hyperfine interactions. As the crystallite size is increased to 20 nm, the sextet pattern emerges at the expense of the doublet as shown in Fig. 10(b). For crystallites of size 30 nm and above, a clear sextet pattern was recorded. The quadruple doublet pattern confirms the magnetisation results that the $CoFe_2O_4$ crystallites below 20 nm are superparamagnetic. Superparamagnetism is characteristic of small crystallites, wherein, the magnetisation is not fixed in any of the easy axes. It is a consequence of the magnetic spins fluctuating among the easy axes of magnetisation in the absence of an external magnetic field. The average time taken for the change of magnetisation from one axis to another is the superparamagnetic relaxation time (τ). Both the

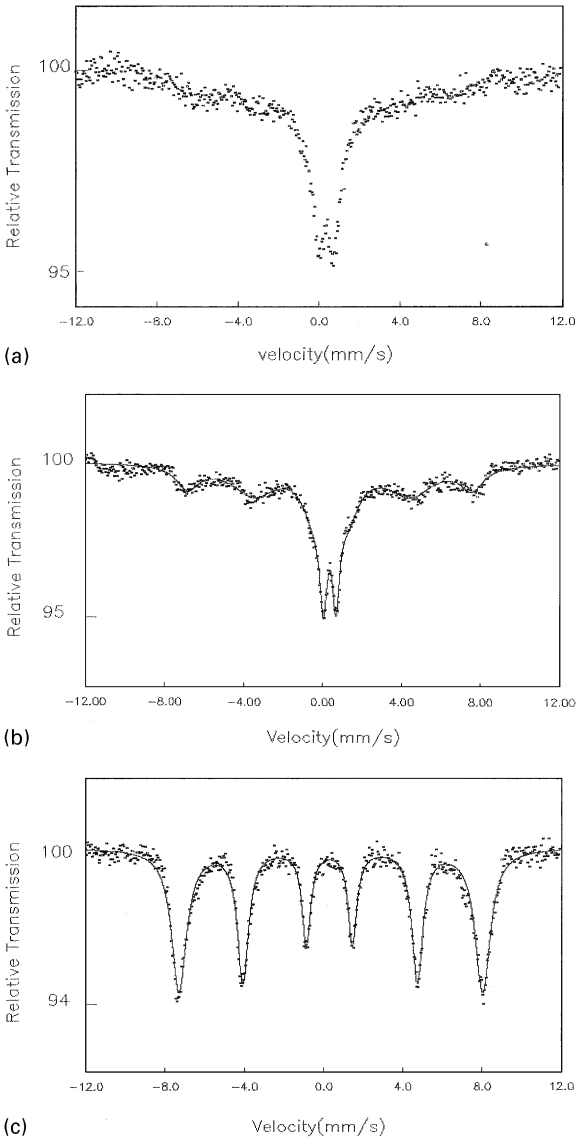

Fig. 10. Mössbauer spectra of nanocrystalline $CoFe_2O_4$ of (a) 6 nm sized (b) 12 nm sized and (c) about 200 nm sized recorded at room temperature.

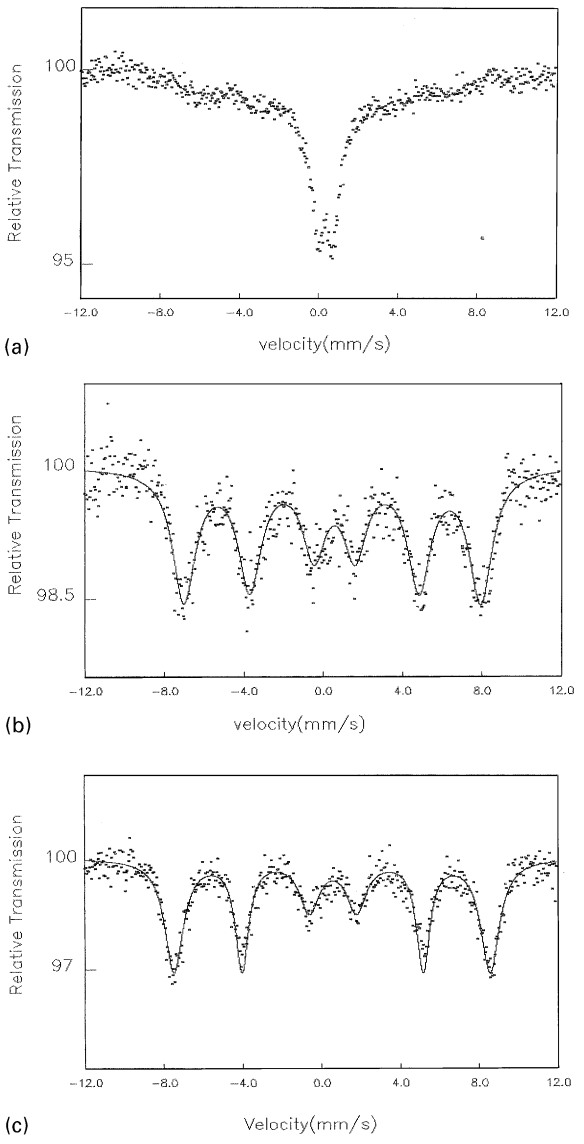

Fig. 11. Low-temperature Mössbauer spectra of 6 nm sized $CoFe_2O_4$ recorded at (a) 300 K (b) 150 K and (c) 40 K.

crystallite size and temperature determines the relaxation time, τ which is approximated as

$$\tau = \tau_0 \exp(KV/k_B T),$$

where K is the anisotropy constant of the crystallite, V the crystallite volume, k_B the Boltzman constant and T is the temperature. τ_0 is a constant (10^{-10} s). When the temperature is constant, the relaxation time varies as a function of crystallite volume, V and shows changes in the Mössbauer spectra as seen in Fig. 10.

The Mössbauer spectra of 6 nm $CoFe_2O_4$ crystallites as a function of temperature is shown in Fig. 11. As seen from Fig. 11(a), only a doublet pattern is registered at room temperature. When the temperature is decreased to 150 K, a sextet pattern is obtained. The sextet pattern becomes

Table 2
Mossbauer parameters of the nanocrystalline $CoFe_2O_4$ powders

Crystallite size (nm)	Measurement temperature (K)	Site	Isomer shift (mm s^{-1})	Quadruple splitting (mm s^{-1})	H_{int} (kOe)
6	300	Doublet	0.35	0.76	—
6	150	Sextet	0.52	0.10	464
6	77	Sextet	0.54	0.08	489
6	40	Sextet	0.55	0.02	498
20	300	Doublet + Sextet	0.35 0.41	0.64 0.11	— 446
20	150	Sextet	0.49	0.66	487
20	77	Sextet	0.52	0.52	502
20	40	Sextet	0.53	0.69	508
30	300	Sextet	0.34	0.03	470
100	300	Sextet	0.33	0.03	476

well defined by lowering the temperature down to 40 K. The Mössbauer parameters of $CoFe_2O_4$ crystallites as a function of crystallite size and temperature of measurement are shown in Table 2. The variations in the Mössbauer spectra correlates with the relaxation time, the crystallite volume and the temperature as given in the above equation. The experimental Mössbauer measurement time, τ_l of 10^{-8} s corresponds to the Larmor precision time of the ^{57}Fe isotope. For smaller crystallites (below 12 nm) the relaxation time, τ is smaller than the τ_l, the magnetic fluctuation is so rapid that the average of internal magnetic hyperfine field is zero to the ^{57}Fe nucleus. This gives only a doublet pattern. When the temperature is decreased, τ increases and approaches τ_l and this gives a sextet pattern. At this stage, some ^{57}Fe nuclei still experience a rapid superparamagnetic relxation and the doublet pattern persists. By lowering the temperature further, the relaxation in the nanocrystallites are much slower and the spectrum becomes a well defined sextet. The Mössbauer results are in agreement with the magnetisation measurements

4. Conclusions

The crystallite size dependent magnetic properties of cobalt ferrite powders prepared by a redox method have been studied. $CoFe_2O_4$ powders possessing 6 nm sized crystallites were superparamagnetic at room temperature and exhibited a reduced magnetisation value of 9 emu g^{-1}. The average crystallite size was varied up to 20 nm by employing controlled preparation conditions. In addition, by heating the 6 nm sized $CoFe_2O_4$ the average crystallite size was systematically varied to study the structural and magnetic properties. The M_s value increased as a function of average crystallite size, whereas, the coercivity increased to show a maximum and dropped. At 300 K, the 6 nm sized sample was superparamagnetic whereas at 150 K a narrow hysteresis was observed. Systematic variations in M_s, M_r and H_c values as a function of measurement temperature has been recorded for samples having different crystallite sizes. The nanocrystalline $CoFe_2O_4$ obtained by oxidative precipitation at room temperature on thermal annealing at 973 K gave a desirable coercivity (1.42 kOe) and saturation magnetisation (60 emu g^{-1}). The Mössbauer spectra reveals superparamagnetism in crystallites upto 20 nm at room temperature. The low-temperature magnetic and Mössbauer results are provided for $CoFe_2O_4$ having different crystallite sizes.

References

[1] K. Haneda, A.H. Morrish, J. Appl. Phys. 63 (8) (1988) 4258.

[2] N. Moumen, P. Veillet, M.P. Pileni, J. Magn. Magn. Mater. 149 (1995) 67.
[3] V. Blaskov, V. Petkov, V. Rusanov, L.M. Martinez, B. Martinez, J.S. Munoz, M. Mikhov, J. Magn. Magn. Mater. 162 (1996) 331.
[4] V. Pillai, D.O. Shah, J. Magn. Magn. Mater. 163 (1996) 243.
[5] K.J. Davis, S. Wells, S.V. Upadhyay, S.W. Charles, K.M O'Grady, M. El Hilo, T. Meaz, S. Morup, J. Magn. Magn. Mater. 149 (1995) 14.
[6] M. Rajendran, A.K. Bhattacharya, J. Mater. Res. submitted.
[7] B.D. Cullity, Elements of X-ray Diffraction, Addison-Wesley, Reading, MA, 1978, p. 101.
[8] S. Brunauer, P.H. Emmett, E. Teller, J. Amer. Chem. Soc. 60 (1938) 309.
[9] P. Boolchand, G.H. Lemon, W.J. Bresser, R.N. Enzweiler, R. Harris, Rev. Sci. Instr. 66 (4) (1995) 3051.
[10] G. Bate, in: E.P. Wohlfarth (Ed.), Ferromagnetic Materials, Vol. 2, North-Holland, Amsterdam, 1980, p. 431.
[11] M. Rajendran, Ph.D. Thesis, Indian Institute of Science, Bangalore, India, 1992.
[12] K.V.P.M. Safi, A. Gedanken, R. Prozorov, J. Balogh. Chem. Mater. 10 (1998) 3445.
[13] M. El-Hilo, K. O'Grady, R.W. Chantrell, J. Magn. Magn. Mater. 114 (1992) 295.